Desalination and Water Treatment
www.deswater.com

doi: 10.5004/dwt.2023.29449

289 (2023) 228–237
March

Activated carbon nanofibers nonwoven flat sheet for methylene blue dye adsorption: batch and flow-through systems

Basma I. Waisi[a,*], Mustafa H. Al-Furaiji[b], Jeffrey R. McCutcheon[c]

[a]*Department of Chemical Engineering, College of Engineering, University of Baghdad, Baghdad, Iraq, email: basmawaisi@gmail.com*
[b]*Environment and Water Directorate, Ministry of Science and Technology, Baghdad, Iraq, email: : alfuraiji79@gmail.com*
[c]*Department of Chemical and Biomolecular Engineering, Center for Environmental Sciences and Engineering, University of Connecticut, Storrs, CT, email: jeffrey.mccutcheon@uconn.edu*

Received 6 October 2022; Accepted 1 March 2023

ABSTRACT

In this study, a flat sheet of electrospun activated carbon nonwoven nanofiber (ACN) based on polyacrylonitrile polymer was fabricated and characterized by Fourier-transform infrared spectroscopy, scanning electron microscopy (SEM), and Brunauer–Emmett–Teller (BET). The SEM analysis showed that the prepared ACN mat consisted of long and bead-free nonwoven nanofibers with an average diameter of 600 nm. The BET analysis of ACN showed that the pores were mesoporous pores with a size of 3.7 nm and a specific surface area of 450 m^2/g. The obtained ACN was used to evaluate the removal of methylene blue (MB) dye from aqueous medium water using batch and flow-through modes. In batch mode, ACN reveals a removal efficiency of up to 90% at the optimum parameter conditions (i.e., pH 7, 100 mg adsorbents, 10 mg/L initial concentration, and room temperature). The adsorption process was well described by the Freundlich isotherm and pseudo-second-order kinetic model with the highest 24.7 mg/g MB dye adsorption capacity. To investigate the effectivity of the ACN nonwoven sheet in a continuous adsorption system, a novel flow-through cell was designed for using nonwoven nanofiber sheets as an adsorbent. The innovative design allows the feed solution to flow within the nanofiber assembly and thus provides a more reachable surface area and longer residence time. Adsorption experiments showed characteristic breakthrough actions in the flow-through process. The breakpoint period was 40 min to treat 25 mL/h of MB dye solution (10 mg/L) in the flow-through system using one layer of 6 cm of ACN mat. In addition, it was found that breakpoint time increased as feed flow decreased, the bed height increased, and the number of ACN mat layers increased due to increasing adsorption sites.

Keywords: Activated carbon; Adsorption; Nanofiber; Polyacrylonitrile; Methylene blue

1. Introduction

The dye-related industries (e.g., textiles, food, dyeing, printing, and tanning industries) are continuously discharging an immense amount of dye waste into the aquatic environment, which has become a significant threat to human health and the environment [1]. Dyes are commonly regarded as hazardous and also carcinogenic [2]. Methylene blue (MB) is a basic cationic dye that is highly soluble in alcohol and water. Excessive doses of methylene blue have been reported to cause diarrhea, vomiting, nausea, gastritis, abdominal and chest pain, extreme headaches, a lot of sweating, mental fatigue, and methemoglobinemia [3]. As a result, it is essential to remove MB dye from the contaminated wastewater streams before discharge to the environment.

Nowadays, physical, chemical, and biological treatment methods have been widely used to extract MB from aqueous solutions, including membranes [4], photocatalytic

* Corresponding author.

1944-3994/1944-3986 © 2023 Desalination Publications. All rights reserved.

degradation [5], electrochemical degradation [6], oxidative degradation [7], and adsorption [8–12].

Adsorption, among other methods, has the advantages of simple operation, low cost, abundant adsorbent materials, high performance, and fast recycling [13,14]. Large spectra of adsorbent materials have been studied in MB removal from agricultural waste materials to advanced nanomaterials. Banana peels, pumpkin peels, grapes, pomelo, tomatoes, cucumber, kaffir lime, and dragon fruit are some examples of agricultural waste materials that have been converted to activated carbon and assessed for MB removal [15]. Recently, nanomaterials have gained more interest in adsorption research due to their unique properties compared to conventional materials [16,17]. Nanomaterials can be used in adsorption in several ways, such as nanoparticles, nanotubes, and nanofibers, and can absorb dyes, metal ions, and organic and inorganic contaminants [18]. In particular, polymer nanofibers have been considered for water treatment in the last few years. Such nanofibers are directly produced using an electrospinning technique and have many attractive features such as large surface area, small pore size, and a small fiber diameter of less than 500 nm [19].

Electrospun nanofibers have recently been considered for the removal of MB dye. Polyacrylonitrile (PAN) nanofibers were used after carbonization by inert gas (i.e., argon) and then oxidation by a mixture of H_2SO_4/HNO_3 [20]. The oxidized electrospun carbon nanofibers were tested in batch mode in MB adsorption. Poly(styrene-co-acrylonitrile) electrospun nanofibers enhanced with carbonaceous materials (i.e., graphite and carbon nanotubes) were examined in batch mode adsorption of MB [21]. Electrospinning and surface modification was applied to the development of deacetylated cellulose acetate (DA) nanofiber membrane modified with polydopamine (PDA) and tested for the removal of methylene blue from aqueous solution using a batch experiment [22].

All previous studies focused on testing electrospun nanofibers as a dye adsorbent in batch mode operation. Batch experiments in adsorption research are so important for understanding the process of isotherm and kinetics. On the other hand, the analysis of adsorption efficiency in continuous mode is of great importance because it reflects the real conditions in the industry and also provides valuable information for the upscaling of the process. In our previous research, continuous flow through the system with a customized design module was used to test the efficiency of electrospun-activated carbon nanofibers (ACN) in the adsorption of emulsified oil [19].

In this research, MB dye was adsorbed on ACN using a new flow-through system developed for nonwoven sheet adsorbent. The innovative design allows the feed solution to flow within the nanofiber assembly and thus provides a more accessible surface area. The effect of feed flow rate, the height of the ACN mat, and the number of ACN layers was investigated.

2. Materials and methods

2.1. Chemicals and materials

Methylene blue dye (MB) from Sigma-Aldrich was used for the preparation of the adsorbate solution. Polyacrylonitrile (PAN) powder was purchased from Scientific Polymer Products, Inc., (MW avg. 150,000), and dimethylformamide (DMF) as a solvent from Acros Organics to prepare the adsorbent materials. The solution pH was adjusted with HCl (0.1 M) and sodium hydroxide (NaOH) (0.1 M), both were purchased from Fisher Scientific.

2.2. Fabrication of adsorbent mat

The polymeric solution for the electrospinning method was prepared by dissolving 16% wt. PAN in DMF solvent with mechanical mixing at 60°C for a couple of hours. The electrospinning process as described in our previous work [18,23] created a precursor nanofiber nonwoven. The polymer solution was applied to a grounded collector drum 18 cm apart, rotating at 70 rpm, using a 20 gauge needle, utilizing a high voltage of 25 kV.

Sequential thermal treatments convert PAN nanofibers to carbon nanofibers. In an air atmosphere, the nanofibers were stabilized in a muffle furnace (Carbolite) at 270°C for 1 h. The stabilized nanofiber mat was carbonized for 2 h in a tube furnace by heating at 650°C for 2 h in a tube furnace (Lindberg/Blue M, Thermo Scientific) in an inert nitrogen gas.

The ramp rate of carbonization was 3°C/min. The electrospun carbonized nanofibers (ECNFN) were then triggered by steam in the same furnace in an inert nitrogen environment at 750°C for 1 h at a steam flow rate of 60 g/h. The rate of activation of the ramp was 5°C/min. The electrospun-activated carbon nanofibers (ACN) adsorbent was the material generated after activation. To optimize the properties of the ACN produced, the conditions used for the mat manufacturing process in this work were chosen according to our previous study [19].

2.3. Adsorbent characterizations

Field emission scanning electron microscopy (SEM, JEOL JSM 6335F) was used to investigate the surface morphology and fiber size of the fabricated nonwovens. The average fiber size of thirty separated fibers was calculated using ImageJ software (National Institutes of Health, USA). The adsorption characteristics of the mat were evaluated using the Brunauer–Emmett–Teller (BET) and Barrett–Joyner–Halenda (BJH) models by the surface area and pore size analyzer (Micromeritics Instrument Corporation). Functional groups on the prepared nanofibers were analyzed using Fourier-transform infrared spectroscopy (FTIR; Perkin Elmer Spectrum RX1 FTIR Spectrometer) and were recorded in the wavenumber range of 500–4,000 cm^{-1} with a resolution of 4 cm^{-1}.

2.4. Adsorption experiments

2.4.1. Batch adsorption experiments

A stock solution of 50 mg/L of MB dye concentration was prepared and various concentrations were collected from a sequence of dilutions. Solutions of 0.1 M NaOH and 0.1 M HCl were used to adjust the pH of the solutions. Batch tests were conducted using 100 mg of ACN in 250 mL of MB solution with an initial concentration of 10 mg/L in a beaker

using a magnetic stirrer at room temperature. The control method (without adsorbent) was performed to ensure that the dye was not ingested into the walls of the beaker. The dimensions of the nonwoven coupons of the ACN were 3 by 3 cm. More information on the setup of the tests has been provided in our previous work [19].

The pH influence was investigated by varying pH values within the range of 3–9. The initial concentration influence was determined by selecting an initial concentration of MB between 10 and 30 mg/L. The effect of the agitation rate was studied at 200, 300, and 400 rpm values. The effect of the adsorption parameters has been elevated by changing one factor at a time while keeping the others constant.

The residual dye concentration was analyzed by UV-Vis spectrophotometer at a wavelength of 650 nm. Percent of removal was calculated using the following equation:

$$\%\text{Removal} = \frac{C_0 - C_e}{C_0} \times 100 \quad (1)$$

where C_0 and C_e are the initial and final concentrations of MB dye (mg/L), respectively. During the experiment, the concentrations of dye were measured at different time intervals. The amount of adsorption at time t (q_t) (mg/g) was calculated using the following equation:

$$q_t = \frac{\left(C_0 - C_t\right)}{m} \times V \quad (2)$$

where C_t is the concentration of MB dye in the solution at time t (mg/L), m is the mass of ACN adsorbent (g), and V is the volume of solution (L).

2.4.2. Fixed bed experiments

A column study was conducted using a cross-section flow system as shown in the schematic diagram in Fig. 1. The system included a flow cell, a syringe pump (KD Scientific), a monolithic quartz glass cell for flow-through measurement, and a UV detector (Model GENESYS 10S UV-Vis) to detect dye concentration in on-line permeate flow using VISION lite software.

The cross-section flow adsorption cell concept seen in Fig. 2 is a novel concept that enables the feed solution to move across the cross-section of the nonwoven mat. The designed adsorption cell was composed of two similarly sized sections of visible acrylic material (12 cm in height, 6 cm in width, and 1 cm in thickness). One of the sections has a flow entrance with a diameter of 3 cm. The location of the exit point is in the downstream portion of the cell. The idea of this design allows a high depth of bed without the need to stack hundreds of coupons on top of each other. A 3 cm × 6 cm mat was fixed between the two sides of the flow-through adsorption cell. A thin gasket and Teflon tape were used as guides to fix the channel height at the thickness of the ACN sheet. The cell was sealed using screws.

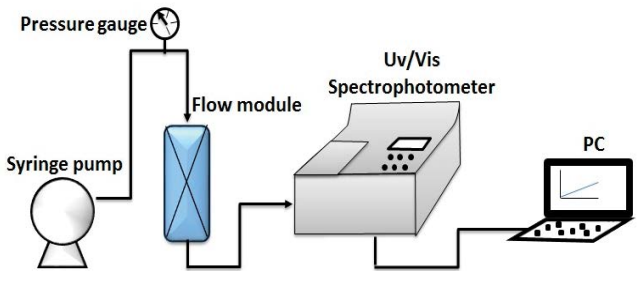

Fig. 1. Schematic diagram of the flow-through adsorption system.

3. Results and discussion

3.1. Adsorbent characterizations

The ACN membrane sheet was characterized by SEM for the observation of the surface and cross-section morphologies presented in Fig. 3A and B, respectively. Activated carbon nanofibers obtained from PAN are long and bead-free with a nonwoven structure. The cross-section morphology image showed an ACN mat thickness of 150 μm. Furthermore, Fig. 3C presents the ACN histogram using the ImageJ analysis software. It can be seen that the nanofiber diameter was between 450 and 750 nm, confirming the uniformity of the nanofiber size of the fabricated ACN with an average diameter of 600 nm.

Fig. 4A presents the N_2 adsorption isotherm of the fabricated ACN as the relative pressure (P/P^0) increases. Adsorption isotherm ACN applies to moderate N_2 adsorption at $P/P^0 < 0.1$ and persistent rise in N_2 adsorption with an improvement across the area of $0.1 < P/P^0 < 0.9$.

The International Union of Pure and Applied Chemistry (IUPAC) categorized adsorbent pores into three groups: micropores (diameter < 2 nm), mesopores (2–50 nm), and macropores (>50 nm) [24]. Thus, depending on the form of the N_2 adsorption isotherm curve, ACN is graded as Type II by IUPAC, reflecting micro and mesopore structures compatible with our previous work [19,25].

Fig. 4B presents BJH adsorption average pore diameter showing that ACN has pores of a diameter between 1.7 and 180 nm in which pore sizes are predominantly micro and mesoporous. 85% of the overall pore volume comes from micro and mesoporous pores with a diameter ranging from

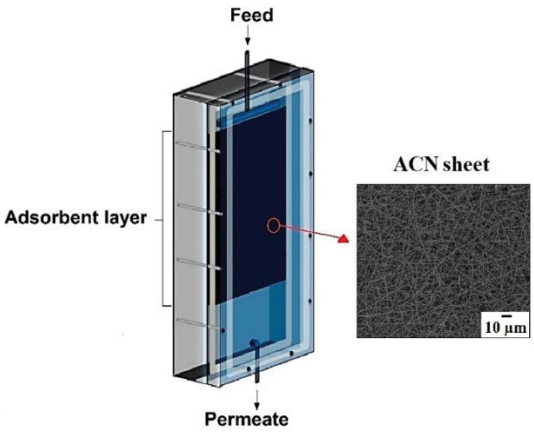

Fig. 2. Schematic graph of the flow-through module design.

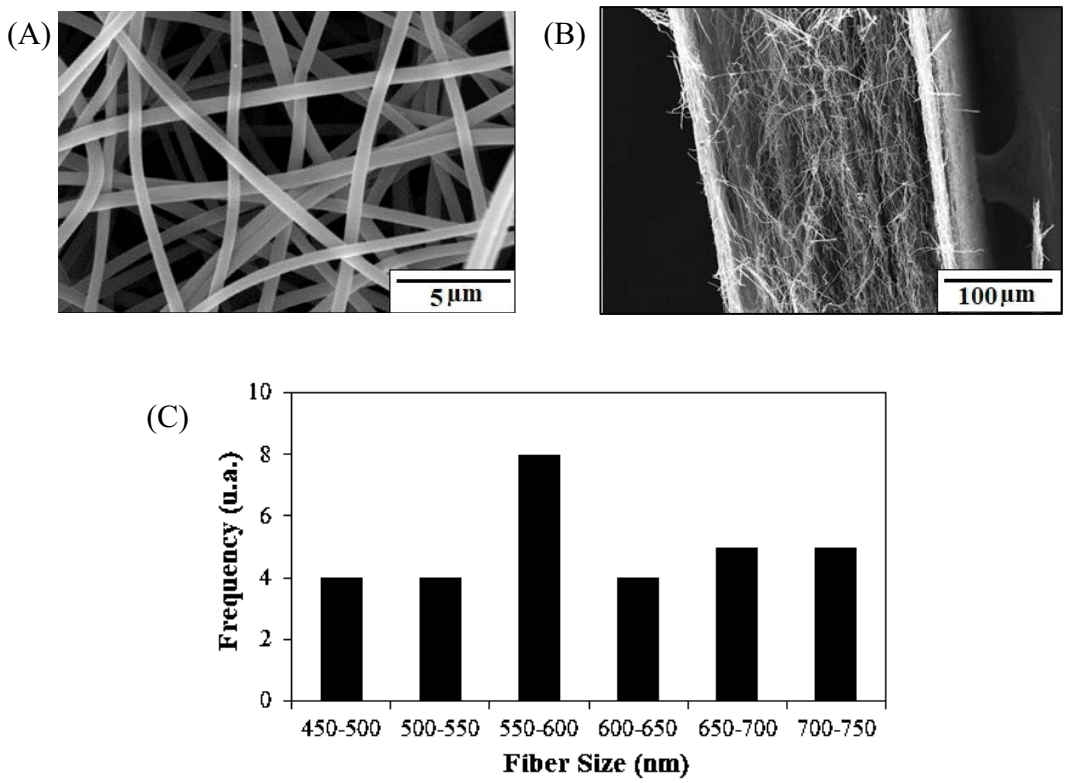

Fig. 3. Morphology characterization of activated carbon nanofibers: (A) scanning electron microscopy surface morphology images, (B) scanning electron microscopy cross-section images, and (C) distribution of fiber sizes.

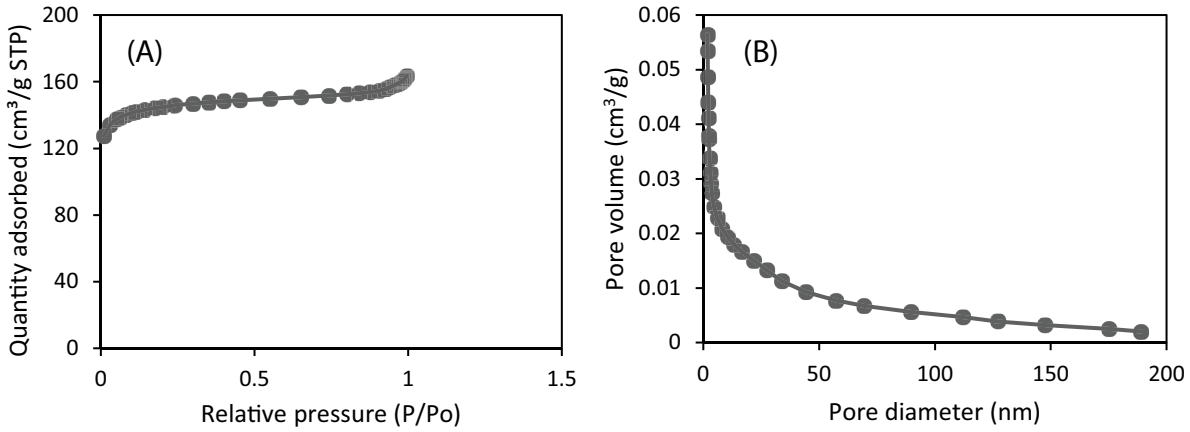

Fig. 4. Adsorption isotherm analysis of the activated carbon nanofibers (A) N_2 adsorption isotherm and (B) pore size distribution.

approximately 1.7–50 nm. The average pore depth, surface area, and overall pore volume of ACN were 3.7 nm, 450 m^2/g, and 0.056448 cm^3/g, respectively. BJH adsorption average pore width was 2.67 nm.

To determine the surface features of the ACN adsorbent mat, the FTIR spectrum curve was carried out in a range of 400–4,000 cm^{-1} as shown in Fig. 5A. The main functional peak groups are 1,160; 1,235 and 1,573.8 cm^{-1} for the (O–H bond in the phenolic group) and carbonyl groups due to steam activation [18,26]. The peak at 1,590 and 1,737.8 cm^{-1} are for the groups C=N and C=O [27]. A small peak of 2,927 cm^{-1} was assigned to the symmetrical stretching vibration of C–H [24]. Fig. 5B shows the surface feature of ACN after MB dye adsorption, most of the surface functional groups in the adsorbent disappeared or decreased due to the cat ion group of MB dye adsorption.

3.2. Batch adsorption experiments

3.2.1. Effect of pH

The initial pH of the adsorbate solution has a significant effect on the ionization degree of the adsorbent molecule

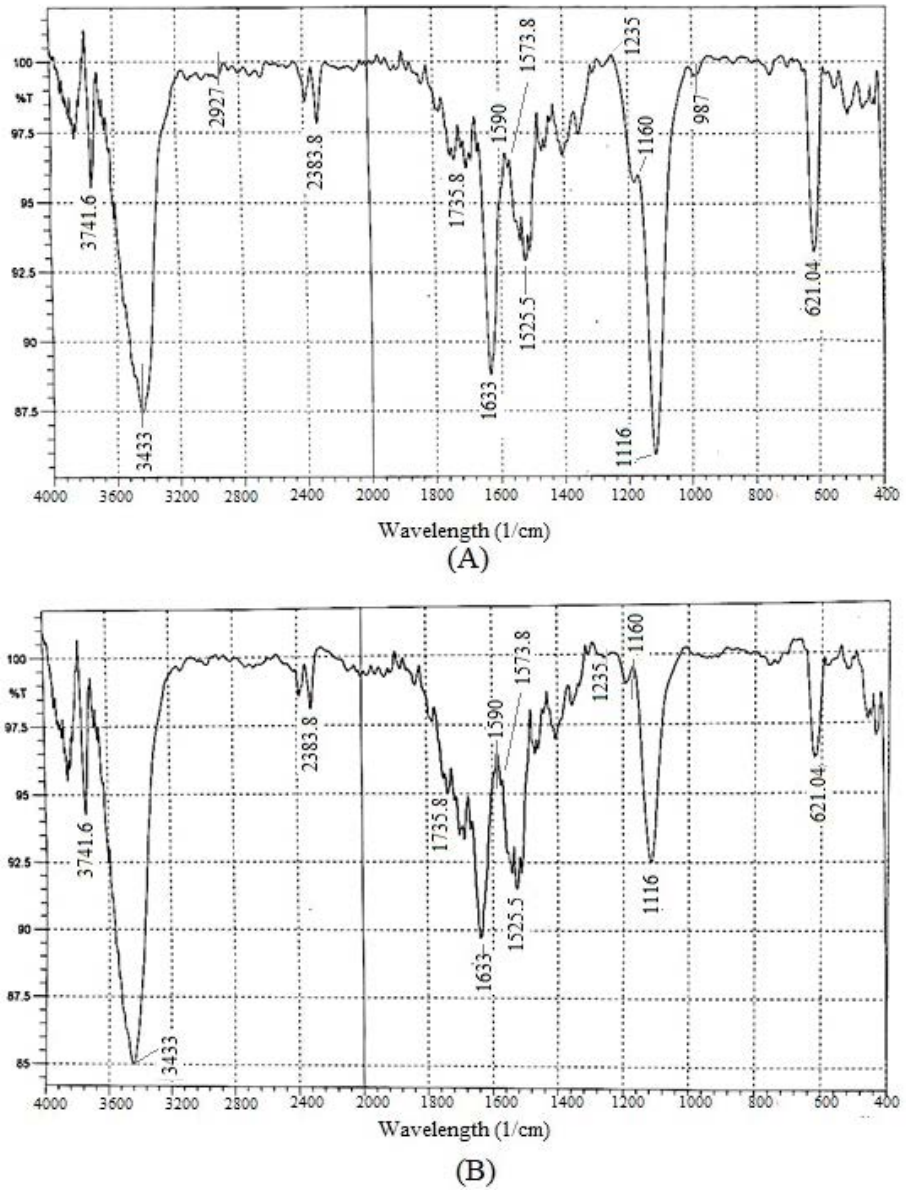

Fig. 5. Fourier-transform infrared spectrophotometer of the activated carbon nanofibers surface (A) before dye adsorption and (B) after dye adsorption.

and the adsorbent properties [28]. The effect of the initial pH of MB dye adsorption on ACN (Fig. 6) was studied by adjusting the precise values of the initial pH solution: 3.0 to 9.0 by adding a few drops of hydrochloric acid (0.1 M) or sodium hydroxide (0.1 M). The efficacy of MB dye removal on ACN showed a clear increase from 30 to more than 90%, with the initial pH values increasing from 3 to 7. However, at pH more than 7, the MB dye adsorption significantly decreased to 20% at pH = 9.

To understand the adsorption mechanism, it is important to determine the zero charge point (pH_{pzc}) which is an indicator of the pH sensitivity and the type of surface active sites of the used adsorbent material. The (pH_{pzc}) corresponds to the pH value for which the net charge of the adsorbent surface is zero because the adsorption depends not only on the Van der Waals forces but also on the electrostatic attractions. The (pH_{pzc}) was determined by a simple electrochemical method [2], by adding 50 mL of sodium chloride (0.05 M) to a series of beakers, the pH of each was adjusted to precise values of pH_i from 2 to 12, then 50 mg of ACN adsorbent was added to each beaker. The samples were agitated at ambient temperature for 48 h and then the final pH was measured to represent the pH_f. The pH_{pzc} is the point where the (pH_f–pH_i) is equal to zero.

The value of pH_{pzc} of the used ACN adsorbent was 7.1, which means that the ACN surface at pH < 7.1 is positively charged and the H^+ ions present at high concentrations compete with the cationic MB dye molecules on the ACN surface for active sites and resulting in the repulsion of the cationic molecules. However, the ACN surface at pH = 7.1

is negatively charged and the MB dye cations are easily adsorbed to negative charges of the OH^- group on the surface of the ACN by electrostatic attraction forces. Beyond this pH value, the removal efficiency decreased sharply due to the presence of additional OH^- ions in the solution that hindered the diffusion of MB dye cations. The maximum uptake of the MB dye on the ACN was at 7 ± 0.1 pH, which was selected as the optimum value in all experiments.

3.2.2. Effect of agitation rate

Fig. 7 displays the impact of the agitation speed on dye removal. The percentage of dye removal increases with an increase in agitation speed. The same behavior was observed for MB dye adsorption by other researchers using carbonized bamboo leaves powder treated with citric acid [29]. It demonstrates the impact of the external mass transport resistance on the kinetics of the adsorption process. Raising the rotating speed conforms to a rise in the Reynolds number and Sherwood number resulting in a higher mass transfer coefficient. The used stirrer speed in the batch experiments in this study was 300 rpm which was good for efficient dye removal.

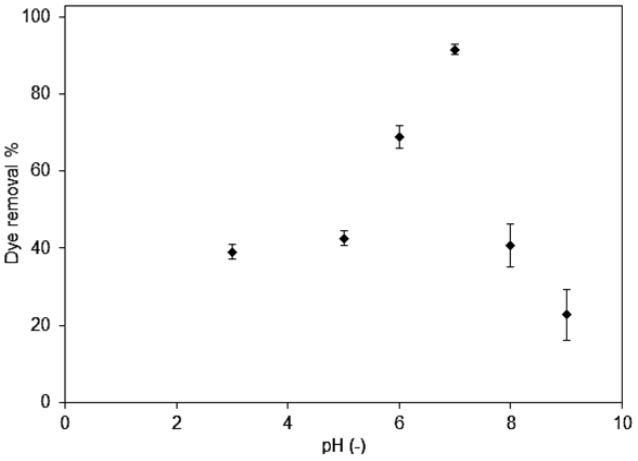

Fig. 6. Effect of the initial pH solution on the adsorption process. All tests were conducted at 25°C, initial dye concentration of 10 mg/L, 100 mg activated carbon nanofibers, agitation rate of 300 rpm, and 250 mL solution.

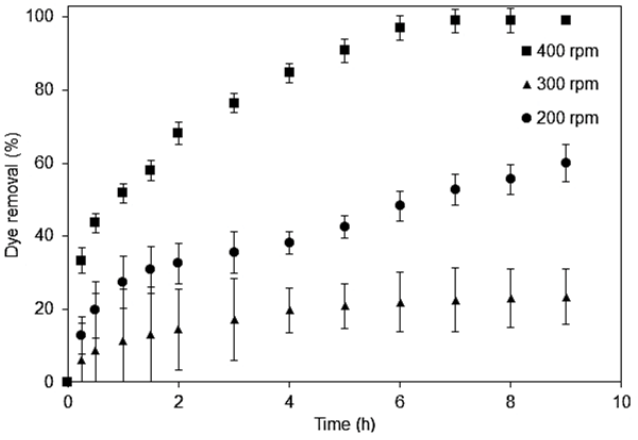

Fig. 7. Effect of agitation rate on the process of adsorption. All experiments were carried out at 25°C, 100 mg activated carbon nanofibers, 10 mg/L initial concentration of methylene blue dye, 250 mL solution, and 7 pH.

3.2.3. Effect of contact time and dye concentration

Fig. 8 illustrates the removal of MB dye by ACN overtime at 25°C at different initial MB dye concentrations. For the different initial concentrations of dye, the plot shows an increase in the percentage of dye removal over time. At the initial concentration of MB dye 10 mg/L, the removal of MB increased sharply to 85% at 5 h, and then the rise became gradual and finally reached 90% at 7 h of contact time.

The dynamics for higher initial concentrations have been distinct. For the initial MB dye concentrations of 20 and 30 mg/L, the adsorbent surface reached an adsorbate equilibrium concentration of 11% and 7%, respectively, at a contact time of 30 min. Most sorption sites are occupied early because the initial concentration is high.

3.2.4. Adsorption isotherm

Adsorption isotherms are crucial for optimizing the use of adsorbents when describing the distribution of adsorbates and the interaction between adsorbates and adsorbents. Besides, adsorption isotherms are important for the determination of the equilibrium concentrations of adsorbate in the solid phase (q_e) and the liquid phase (C_e) [30,31]. Adsorption isotherms in liquid and solid phases are often used as Langmuir and Freundlich isotherm models.

The Langmuir isotherm has been extensively used to explain single-solute systems by assuming localized adsorption on the external surface of the adsorbent without interaction between molecules adsorbed on neighboring sites. This model assumes that the adsorption process homogeneously takes place at different sites that produce a single

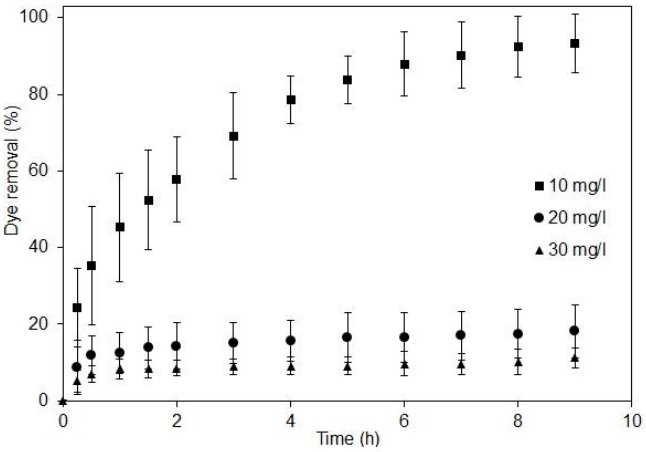

Fig. 8. Effect of the initial methylene blue dye concentration in the adsorbate solution on the adsorption process. All experiments were performed at 25°C, 100 mg activated carbon nanofibers, 300 rpm agitation rate, and 250 mL solution.

absorbing layer [32]. The linear form of the Langmuir isotherm can be described in the following equation:

$$\frac{C_e}{q_e} = \frac{1}{q_{\max} b} + \frac{C_e}{q_{\max}} \tag{3}$$

where q_e is a solid phase dye concentration at equilibrium (mg/g), $q_{\max}$ is the maximum adsorption capacity (mg/g) and b is the Langmuir isothermal equilibrium constant associated with adsorption energy (L/mg) [39]. Such values can be found by plotting C_e/q_e against C_e. A higher b value is a criterion for the propensity of the adsorbate to adsorb the active sites of the adsorbent surface reflecting higher adsorption strength. In the current research, the adsorption method suits well with the Langmuir model with a correlation coefficient of $R^2 > 0.99$. Also, the high value of b (as seen in Table 1) shows the high affinity of the MB dye molecules to the ACN nonwoven mat. Also, the adsorption efficiency and usability of the Langmuir equation can be evaluated using the separation factor (R_L) value estimated by the following equation:

$$R_L = \frac{1}{1 + bC_0} \tag{4}$$

where R_L values between 0 and 1 indicate favorable adsorption, while $R_L = 0$, $R_L = 1$, and $R_L > 1$ indicate irreversible, linear, and unfavorable adsorption processes, respectively. The R_L value in this study was 3.3×10^{-3}, indicating a favorable adsorption process.

The Freundlich isotherm model is an empirical equation that can be applied to multilayer adsorption, assuming heterogeneous active sites on the surface of the adsorbent. This means that an increase in the concentration of adsorbate leads to an increase in the concentration of adsorbate on the adsorbent surface. The linear form of the Freundlich isotherm model is written as follows:

$$\ln q_e = \ln K_f + \frac{1}{n} \ln C_e \tag{5}$$

where K_f and $1/n$ are the Freundlich isotherm constants indicating the extent of the adsorption and the degree of surface heterogeneity of the non-linearity between the concentration of the solution and the adsorption, respectively.

Table 1 describes the fitting parameters of the Langmuir and Freundlich equations for the adsorption of the MB dye molecules to the ACN sheet. The low value of K_f indicates the low adsorption rate, while the value of $1/n$ between 0 and 1 indicates unfavorable adsorption [33–35]. As a consequence, the MB dye adsorption on the ACN is fitted with the Langmuir isothermal model, which means that monolayer adsorption occurs under the experimental conditions of this study.

Table 1
Langmuir and Freundlich isotherm constants and error analysis

Langmuir		Freundlich	
$q_{\max}$ (mg/g)	13.6986	K_f (mg/g)	2.57
b (L/mg)	30.4167	$1/n$	0.0354
R^2_L	0.9997	R^2_F	0.9870

3.2.5. Adsorption kinetics

Adsorption kinetics is important to predict the rate of adsorption and to establish an effective treatment method based on the adsorption process. Pseudo-first-order and pseudo-second-order models are most widely used to explain the adsorption kinetics. The following expression can be used for the pseudo-first-order model:

$$\ln\left(q_e - q_t\right) = \ln q_e - k_1 t \tag{6}$$

where q_t is the amount of dye adsorbed at time t (mg/g), k_1 is the pseudo-first-order constant (h^{-1}). The rate of the pseudo-first-order model is influenced by the quantity of dye molecules adsorbed at equilibrium.

The other kinetic model is the pseudo-second-order model which is given as follows:

$$\frac{t}{q_t} = \frac{1}{k_2 q_e^2} + \frac{t}{q_e} \tag{7}$$

where k_2 is the rate constant of the second-order equation (g/mg·h).

The kinetics parameters of the pseudo-first-order and pseudo-second-order models of MB dye adsorption are shown in Table 2. Correlation coefficients, R^2 for pseudo-first-order, and pseudo-second-order models were 0.979 and 0.985, respectively.

3.3. Fixed-bed adsorption

3.3.1. Flow rate effect

Results for different feed flow rates are shown in Fig. 9 with one layer of 6 cm ACN bed height and an inlet dye concentration of 10 mg/L. Fig. 11 indicates an increase in the slope of the break-through curve with the feed flow rate. By using a feed flow rate of 75 mL/h, the concentration of MB dye in the water in the outlet water stream reached the initial concentration faster than using a feed flow rate of 50 or 25 mL/h. The residence time of the dye molecules in the nanofiber mat was too short to occupy all the adsorption sites contributing to an earlier breakthrough stage.

Using this new design of the flow-through adsorption cell has helped to allow the feed solution to flow through the cross-section of the ACN mat along the direction of the

Table 2
Pseudo-first-order and pseudo-second-order kinetic models constants and error analysis

Pseudo-first-order		Pseudo-second-order	
$q_{e,\text{cal}}$ (mg/g)	23.0116	$q_{e,\text{cal}}$ (mg/g)	25.5102
k_1 (h^{-1})	0.4928	k_2 (g/mg·h)	0.03851
R^2_1	0.9793	R^2_2	0.9842

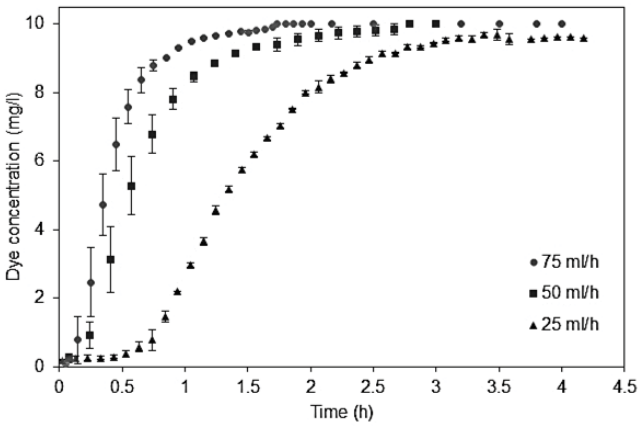

Fig. 9. Impact of flow rate on flow-through adsorption process through activated carbon nanofibers mat (6 cm of 1 layer). All experiments were conducted at 25°C, with an initial methylene blue dye concentration of 10 mg/L and a pH of 7.

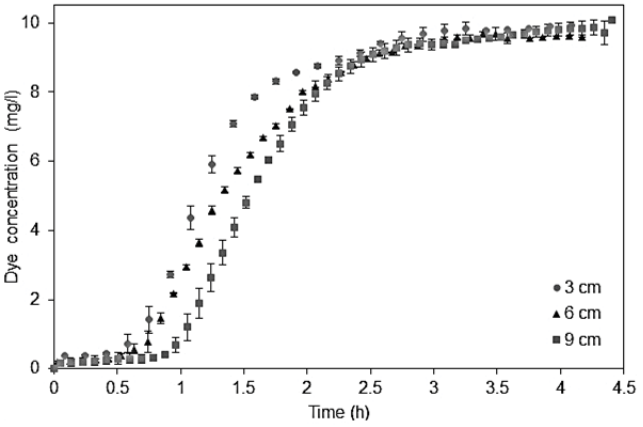

Fig. 10. Effect of bed height on flow through the adsorption process. All tests were performed at 25°C with a feed flow rate of 25 mL/h, an initial methylene blue dye concentration of 10 mg/L, and a pH of 7.

nanofibers within the nonwoven structure. As a result, the surface of the nanofibers was completely exposed to the dye solution. Most of the dye molecules were adsorbed at the adsorption sites along the nanofiber surface of the ACN. When the adsorption sites were occupied, the dye molecules began to discharge with the effluent.

3.3.2. Bed height effect

To evaluate the effect of bed height on MB dye removal in the flow-through system, the height of the ACN mat was changed. As shown in Fig. 10, using 3, 6, and 9 cm of ACN mat led to a marked difference in breakthrough time. The increase in bed height, which is directly related to bed mass, makes it easier to handle a greater amount of feed solution. When the height of the bed increases, more resident time in the bed and more adsorption sites are available for dye adsorption on nanofiber surface s resulting in enhanced efficiency of dye removal.

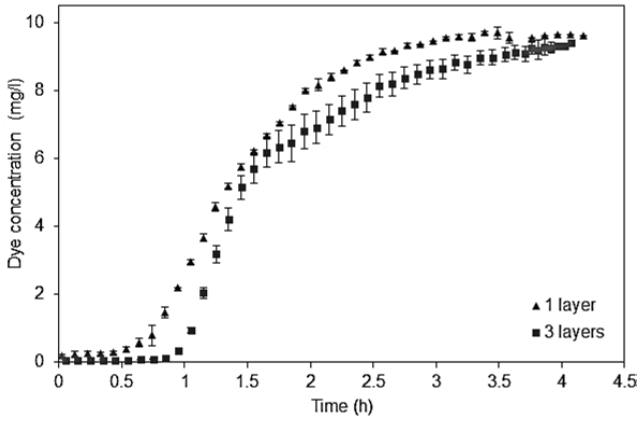

Fig. 11. Effect of numbers of activated carbon nanofibers layer on flow through the adsorption process. All experiments were conducted at 25°C, 6 cm of activated carbon nanofibers, the feed flow rate was 25 mL/h, initial methylene blue dye concentration of 10 mg/L, and pH 7.

3.3.3. Number of layers

The number of ACN layers reflects the thickness of the mat membrane. Fig. 11 demonstrates the change in the concentration of permeate dye over time using 1 and 3 layers of ACN. Using more layers of ACN, improved the efficiency of the removal of the dye and increased the breakthrough time. The noticeable improvement in efficiency can be explained by an increase in the fiber quantity in the beds and adsorption sites.

4. Conclusion

In this research, it has been confirmed that electrospun ACN nonwoven membrane derived from PAN can be used effectively for methylene blue (MB) dye adsorption from wastewater. The fabricated nonwoven nanofibers are long, bead-free, and smooth with unique properties such as high specific surface area (i.e., 450 m^2/g) and micro and mesoporous structure and thus they exhibit a high efficiency for MB dye removal. In batch experiments, the MB dye removal rate is highly dependent on the initial pH value. The maximum adsorbing rate of the MB dye on the ACN was on a pH of 7.1 which was selected as the optimal value with achieving a 90% removal percentage. MB dye removal fits well with the Langmuir isotherm and pseudo-second-order models.

The new design flow-through cell was used to study the flow-through performance characteristics of the ACN membrane sheet to remove MB dye from wastewater. The results showed a significant impact on the MB dye removal efficiency of the bed height, the number of ACN membrane layers, and the flow rate. At a 10 mg/L of initial MB dye concentration, 6 cm of bed height, 3 layers of ACN membrane mat, and a flow rate of 25 mL/h, the break-through point was 1 h. the efficacy of MB dye removal using the new flow-through cell increases with increasing the height and number of adsorbent sheets due to increasing the adsorption sites and the contact time. It is found that the novel design packed bed is an effective method to use the ACN

membrane sheet for MB dye removal from water in a flow-through system. It is recommended to study the efficiency of this new design in removing other pollutants such as heavy metals, oil, phenol, and other organic contaminants.

Acknowledgments

The authors would like to thank the Higher Committee for Education Development (HCED) in Iraq for their financial support (Grant Number 1000324). Also, the authors are grateful to the Center for Clean Energy Engineering at the University of Connecticut for using the nitrogen adsorption analyzer.

References

[1] E. Santoso, R. Ediati, Y. Kusumawati, H. Bahruji, D.O. Sulistiono, D. Prasetyoko, Review on recent advances of carbon based adsorbent for methylene blue removal from waste water, Mater. Today Chem., 16 (2020) 100233, doi: 10.1016/j.mtchem.2019.100233.

[2] O.A.A. Mahmood, B.I. Waisi, Synthesis and characterization of polyacrylonitrile based precursor beads for the removal of the dye malachite green from its aqueous solutions, Desal. Water Treat., 216 (2021) 445–455.

[3] R. Wijaya, G. Andersan, S. Permatasari Santoso, W. Irawaty, Green reduction of graphene oxide using kaffir lime peel extract (*Citrus hystrix*) and its application as adsorbent for methylene blue, Sci. Rep., 10 (2020) 1–9, doi: 10.1038/s41598-020-57433-9.

[4] A.K. Shukla, J. Alam, M. Rahaman, A. Alrehaili, M. Alhoshan, A. Aldalbahi, A facile approach for elimination of electroneutral/anionic organic dyes from water using a developed carbon-based polymer nanocomposite membrane, Water Air Soil Pollut., 231 (2020) 104, doi: 10.1007/s11270-020-04483-4.

[5] A. Geng, Y. Zhang, X. Xu, H. Bi, J. Zhu, Photocatalytic degradation of organic dyes on Li-doped graphitic carbon nitrides, J. Mater. Sci. - Mater. Electron., 31 (2020) 3869–3875.

[6] M.H. Abdel-Aziz, M. Bassyouni, M.S. Zoromba, A.A. Alshehri, Removal of dyes from waste solutions by anodic oxidation on an array of horizontal graphite rods anodes, Ind. Eng. Chem. Res., 58 (2019) 1004–1018.

[7] G. Son, D. Hyung Kim, J.S. Lee, H. Lee, Enhanced methylene blue oxidative removal by copper electrode-based plasma irradiation with the addition of hydrogen peroxide, Chemosphere, 157 (2016) 271–275.

[8] A.P. Rawat, V. Kumar, D.P. Singh, A combined effect of adsorption and reduction potential of biochar derived from Mentha plant waste on removal of methylene blue dye from aqueous solution, Sep. Sci. Technol., 55 (2020) 907–921.

[9] S.M. Wabaidur, M.A. Khan, M.R. Siddiqui, M. Otero, B.-H. Jeon, Z.A. Alothman, A.A. Hussain Hakami, Oxygenated functionalities enriched MWCNTs decorated with silica coated spinel ferrite – a nanocomposite for potentially rapid and efficient de-colorization of aquatic environment, J. Mol. Liq., 317 (2020) 113916, doi: 10.1016/j.molliq.2020.113916.

[10] S.A. Alshareef, M. Otero, H.S. Alanazi, M.R. Siddiquia, M.A. Khan, Z.A. Alothman, Upcycling olive oil cake through wet torrefaction to produce hydrochar for water decontamination, Chem. Eng. Res. Des., 170 (2021) 13–22.

[11] V. Sasidharan, J. Georgin, D.S.P. Franco, L. Meili, P. Singh, A.H. Jawad, R. Selvasembian, Correction to: hexavalent chromium adsorption onto environmentally friendly mesquite gum-based polyurethane foam, Biomass Convers. Biorefin., (2022) 13399, doi: 10.1007/s13399-022-03703-7.

[12] K.F.A. Zahari, U.K. Sahu, T. Khadiran, S.N. Surip, Z.A. ALOthman, A.H. Jawad, Mesoporous activated carbon from bamboo waste via microwave-assisted K_2CO_3 activation: adsorption optimization and mechanism for methylene blue dye, Separations, 9 (2022) 390, doi: 10.3390/separations9120390.

[13] R. Gusain, N. Kumar, S.S. Ray, Recent advances in carbon nanomaterial-based adsorbents for water purification, Coord. Chem. Rev., 405 (2020) 213111, doi: 10.1016/j.ccr.2019.213111.

[14] M. Bardhan, T.M. Novera, M. Tabassum, A. Islam, A.H. Jawad, A. Islam, Adsorption of methylene blue onto betel nut husk-based activated carbon prepared by sodium hydroxide activation process, Water Sci. Technol., 82 (2020) 1932–1949.

[15] M. Kadhom, N. Albayati, H. Alalwan, M. Al-Furaiji, Removal of dyes by agricultural waste, Sustainable Chem. Pharm., 16 (2020) 100259, doi: 10.1016/j.scp.2020.100259.

[16] B.I. Waisi, S.M. Al-jubouri, R. Mccutcheon, Fabrication and characterizations of silica nanoparticle embedded carbon nanofibers, Ind. Eng. Chem. Res., 58 (2019) 4462–4467.

[17] B.I. Waisi, Carbonized copolymers nonwoven nanofibers composite : surface morphology and fibers orientation, Iraqi J. Chem. Pet. Eng., 20 (2019) 11–15.

[18] B.I. Waisi, S.S. Manickam, N.E. Benes, A. Nijmeijer, J.R. McCutcheon, Activated carbon nanofiber nonwovens: improving strength and surface area by tuning the fabrication procedure, Ind. Eng. Chem. Res., 58 (2019) 4084–4089.

[19] B.I. Waisi, J.T. Arena, N.E. Benes, A. Nijmeijer, J.R. McCutcheon, Activated carbon nanofiber nonwoven for removal of emulsified oil from water, Microporous Mesoporous Mater., 296 (2020) 109966, doi: 10.1016/j.micromeso.2019.109966.

[20] B.M. Thamer, H. El-Hamshary, S.S. Al-Deyab, M.H. El-Newehy, Functionalized electrospun carbon nanofibers for removal of cationic dye, Arabian J. Chem., 12 (2019) 747–759.

[21] A.A. Elzain, M.R. El-Aassar, F.S. Hashem, F.M. Mohamed, A.S.M. Ali, Removal of methylene dye using composites of poly(styrene-co-acrylonitrile) nanofibers impregnated with adsorbent materials, J. Mol. Liq., 291 (2019) 111335, doi: 10.1016/j.molliq.2019.111335.

[22] J. Cheng, C. Zhan, J. Wu, Z. Cui, J. Si, Q. Wang, X. Peng, L.-S. Turng, Highly efficient removal of methylene blue dye from an aqueous solution using cellulose acetate nanofibrous membranes modified by polydopamine, ACS Omega, 5 (2020) 5389–5400.

[23] S.M. Alkarbouly, B.I. Waisi, Fabrication of electrospun nanofibers membrane for emulsified oil removal from oily wastewater, Baghdad Sci. J., 19 (2022) 1238–1248.

[24] J.-J. Gao, Y.-B. Qin, T. Zhou, D.-D. Cao, P. Xu, D. Hochstetter, Y.-F. Wang, Adsorption of methylene blue onto activated carbon produced from tea (*Camellia sinensis* L.) seed shells: kinetics, equilibrium, and thermodynamics studies, J. Zhejiang Univ. Sci. B, 14 (2013) 650–658.

[25] S.S. Manickam, U. Karra, L. Huang, N. Bui, B. Li, J.R. McCutcheon, Activated carbon nanofiber anodes for microbial fuel cells, Carbon N. Y., 53 (2013) 19–28.

[26] K.L. Klein, A.V. Melechko, T.E. McKnight, S.T. Retterer, P.D. Rack, J.D. Fowlkes, D.C. Joy, M.L. Simpson, Surface characterization and functionalization of carbon nanofibers, J. Appl. Phys., 103 (2008), doi: 10.1063/1.2840049.

[27] S.N. Arshad, M. Naraghi, I. Chasiotis, Strong carbon nanofibers from electrospun polyacrylonitrile, Carbon N. Y., 49 (2011) 1710–1719.

[28] E. Bazrafshan, P. Amirian, A.H. Mahvi, A. Ansari-Moghaddam, Application of adsorption process for phenolic compounds removal from aqueous environments: a systematic review, Global NEST J., 18 (2016) 146–163.

[29] S.K. Ghosh, A. Bandyopadhyay, Adsorption of methylene blue onto citric acid treated carbonized bamboo leaves powder: equilibrium, kinetics, thermodynamics analyses, J. Mol. Liq., 248 (2017) 413–424.

[30] V. Gokmen, A. Serpen, Equilibrium and kinetic studies on the adsorption of dark colored compounds from apple juice using adsorbent resin, J. Food Eng., 53 (2002) 221–227.

[31] K.R. Kalash, H.A. Alalwan, M.H. Al-furaiji, A.H. Alminshid, B.I. Waisi, Isothermal and kinetic studies of the adsorption removal of Pb(II), Cu(II), and Ni(II) ions from aqueous solutions using modified *Chara* sp. algae, Korean Chem. Eng. Res., 58 (2020) 301–306.

[32] F.D. Ardejani, K. Badii, N.Y. Limaee, S.Z. Shafaei, A.R. Mirhabibi, Adsorption of Direct Red 80 dye from aqueous

solution onto almond shells: effect of pH, initial concentration and shell type, J. Hazard. Mater., 151 (2008) 730–737.
[33] L. Li, X. Wang, D. Zhang, R. Guo, X. Du, Excellent adsorption of ultraviolet filters using silylated MCM-41 mesoporous materials as adsorbent, Appl. Surf. Sci., 328 (2015) 26–33.
[34] F. Haghseresht, G.Q. Lu, Adsorption characteristics of phenolic compounds onto coal-reject-derived adsorbents, Energy Fuels, 12 (1998) 1100–1107.
[35] J.C. Igwe, A.A. Abia, Adsorption isotherm studies of Cd(II), Pb(II) and Zn(II) ions bioremediation from aqueous solution using unmodified and EDTA-modified maize cob, Eclet. Quim., 32 (2007) 33–42.